Histol Histopathol (2024) 39: 783-794

Histology and Histopathology
From Cell Biology to Tissue Engineering

ORIGINAL ARTICLE Open Access

Clinicopathological analysis of bronchiolar adenoma combined with lung adenocarcinoma: Report of eight cases and literature review

Minsheng Zhu*, Qianqian Yang*, Shenghua Zhan, Weishuo Liu, Wei Liu, Lingchuan Guo and Shan Huang

Department of Pathology, The First Affiliated Hospital of Soochow University, Suzhou, Jiangsu, China

*The two authors contributed equally to this work: Minsheng Zhu, Qianqian Yang

Summary. Aims. To investigate the clinicopathological characteristics and potential diagnostic pitfalls of bronchiolar adenoma (BA) combined with lung adenocarcinoma (LUAD) in the same lesion.

Methods. We analyzed eight cases of BA combined with LUAD from our hospital pathology department between July 2020 and January 2022, and summarized their clinical data, radiological features, histopathological characteristics and immunohistochemical phenotypes.

Results. Upon macroscopic examination, the lesions were characterized by gray-white or gray-brown solid nodules with well-defined borders, measuring 0.6-1.8cm in maximum diameter. The incidence of proximal-type BA (6/8) was higher than that of distal-type BA (2/8), and they combined with different stages of LUAD, including adenocarcinoma *in situ*, minimally invasive adenocarcinoma, invasive adenocarcinoma, and invasive mucinous adenocarcinoma (IMA). Immunohistochemistry showed that cytokeratin 5/6 and P40 were positive in the continuous basal cell layer in BA, but only scattered positive basal cells were seen at the junction of BA and LUAD. TTF-1 was positive in proximal-type BA ciliated cells in five cases and in LUAD cells in seven cases, and weakly positive in some basal cells. One case of IMA and mucinous cells of BA were TTF-1 negative. There was partially positive Napsin-A expression in BA luminal cells and LUAD cells of all cases except IMA.

Conclusion. There is no obvious boundary when BA and LUAD are in the same lesion. The luminal epithelial cells in the area where the two components migrate toward each other are atypical and lack a continuous underlying basal cell layer. Microscopic diagnosis should be aided by immunohistochemistry.

Key words: Malignant potential, Identification, Histopathological features, Immunohistochemistry (IHC), Microscopy diagnosis

Introduction

Bronchiolar adenoma (BA) is a benign tumor of the lungs arising from bronchiolar luminal cells. It is distinguished histologically from lung adenocarcinoma (LUAD) by its double-layered structure consisting of epithelial cell and continuous basal cell layers. The epithelial cell layer of BA consists of varying proportions of mucous cells, ciliated cells, and cuboidal cells that resemble type II pneumocytes (Chang et al., 2018). A recent study redefined BA by dividing it into two major histological subtypes, proximal (myxoid adenoma) and distal (alveolar adenoma), based on morphological similarity to normal bronchiolar branches at various sites (Chang et al., 2018). Luminal cells in proximal-type BA contain abundant cilia and a high proportion of mucous cells. In contrast, luminal cells in distal-type BA show a predominance of cuboidal cells that resemble type II pneumocytes, but ciliated cells and mucous cells are rare or absent. Although the histological characteristics of BA are clear, misdiagnosis still occurs pathologically. In the context of frozen sections diagnosis, the presence of coexisting BA and LUAD may lead to the inadvertent disregard of LUAD

Corresponding Author: Lingchuan Guo or Shan Huang, Department of Pathology, The First Affiliated Hospital of Soochow University, Suzhou, Jiangsu, 215123, China. e-mail: szglc@hotmail.com or goatsz@163.com

www.hh.um.es. DOI: 10.14670/HH-18-682

Abbreviations. BA, Bronchiolar adenomas; LUAD, Lung adenocarcinoma; CMPT, Ciliated muco-nodular papillary tumor; IMA, Invasive mucinous adenocarcinoma; NSCLC, Non-small cells lung cancer; AIS, Adenocarcinoma *in situ*; TTF-1, Thyroid transcription factor-1; CK5/6, Creatine kinase 5/6; CCNE1, Cyclin E1; EGFR, Epidermal growth factor receptor; KRAS, Kirsten rat sarcoma viral oncogene homolog; BRAF, B-Raf proto-oncogene, serine/threonine kinase; IHC, Immunohistochemistry

components or the misdiagnosis of BA as LUAD. There are rare reports suggesting that BA has malignant potential but this remains controversial and unclear (Arai et al., 2010; Miyai et al., 2018; Han et al., 2021; Wang et al., 2021). Based on the histological features observed in the co-occurrence of BA and LUAD within the same lesion, it is hypothesized that BA may undergo a progression towards atypical hyperplasia, ultimately culminating in the development of LUAD.

For patients with BA complicated with early LUAD, surgical resection is sufficient (lung wedge resection), and patients should be followed up regularly after surgery. For patients with invasive adenocarcinoma, surgical resection is the main treatment. When the invasion exceeds 5 mm or the differentiation is poor, pulmonary lobectomy or segmentectomy should be performed. If necessary, postoperative radiotherapy, chemotherapy or molecular targeted therapy should be performed.

Accurate diagnosis of BA combined with LUAD is critical to patient prognosis. In this study, we combined histological features, immunohistochemistry, and molecular pathology to explore BA combined with LUAD, to improve its pathological diagnosis.

Materials and methods

We retrospectively analyzed eight patients with pulmonary nodules who were admitted to the First Affiliated Hospital of Soochow University and underwent partial lung resection between July 2020 and January 2022. The morphological characteristics of resected specimens were analyzed by two experienced pathologists according to the 2021 World Health Organization Classification of Thoracic Tumors.

Preparation of frozen sections: the fresh surgical specimens were placed on the support, and tissue embedding agent was applied to the surrounding area. The embedded tissues were placed on a freezing table for 1-3 minutes until frozen. The frozen tissue blocks were cut into sections of 5-10 μm thickness using a frozen slicer, and the tissue sections were placed on clean glass slides. Finally, the frozen sections were stained with hematoxylin and eosin.

For preparation of paraffin sections, surgical specimens were fixed in 10% neutral buffered formalin, embedded in paraffin, cut into serial 3-4-μm sections, and stained with hematoxylin and eosin.

Preparation of immunohistochemistry (IHC): All surgically resected specimens were fixed in 10% neutral formalin and paraffin-embedded for sectioning. Staining was performed using the EnVision two-step method for immunohistochemistry. Antibodies used for IHC included anti-p40, anti-TTF-1, anti-P63 and anti-Ki-67 (Gene Biology, Shanghai, China), anti-Napsin-A (Zhongshan Jinqiao Biotechnology, Beijing, China), anti-CK5/6 (Dako, Santa Clara, USA). Immunohistochemical staining was performed on a Dako automated instrument (Dako Omnis; Agilent Technologies, Santa Clara, CA, USA) according to the manufacturer's instructions.

Results

Clinical and Radiographic Characteristics

Detailed clinicopathological characteristics of all patients are shown in Table 1. All patients were female, and the median age at the time of diagnostic imaging was 58 years. Seven patients underwent lung wedge resection or segmentectomy, and one underwent lobectomy. Computed tomography revealed that four patients exhibited solitary ground-glass nodules, while three presented with slightly hyperdense nodules, and one case exhibited a mixed density shadow. Additionally, two patients displayed nodules with surrounding pleural traction. Upon gross examination, these nodules ranged in diameter from 0.6 to 1.8 cm with clear borders to the surrounding parenchyma.

Pathological diagnosis of intraoperative frozen section

To determine the extent of surgical resection, we performed intraoperative frozen section examination on the pulmonary nodules. However, the frozen section examination of all lesions was not completely consistent with the final pathological diagnosis with the paraffin sections (Table 1). By frozen section examination, three lesions only had BA, but their final diagnosis was BA combined with minimally invasive adenocarcinoma, BA combined with well-differentiated adenocarcinoma, and BA combined with invasive mucinous adenocarcinoma (IMA). Frozen section examination of the remaining five lesions, including minimally invasive adenocarcinoma (n=2) and LUAD (n=3), missed BA components. The final diagnosis of the first two lesions was BA (proximal type) combined with adenocarcinoma *in situ* (AIS). The latter three lesions were one BA (proximal type) combined with LUAD and two BA (distal type) combined with LUAD.

Characteristics of proximal-type BA combined with LUAD

There were five lesions of proximal-type BA combined with LUAD. The LUAD components in these lesions were two invasive adenocarcinomas, two minimally invasive adenocarcinomas, and one AIS. Proximal-type BA was classified into ciliated muconodular papillary tumor (CMPT) characterized by prominent papillary architecture and glandular-based flat type. Both were lined with abundant ciliated columnar cells and a high proportion of mucous cells, and the glandular lumen was rich in mucus (Fig. 1A,B). A small amount of micropapillary morphology was observed in papillary BA, which needed to be differentiated from the micropapillary subtype in adenocarcinoma. However, close inspection of the former revealed ciliated cells on the luminal surface, with a continuous basal cell layer

beneath these luminal cells. The region of minimally invasive adenocarcinoma showed cells with a hobnail appearance protruding into the alveolar lumen, and the invasive area was dominated by glandular architecture. The luminal cells had moderate to severe atypia, but ciliated cells and basal cell layers were absent (Fig. 1C). Notably, there was one case of BA combined with well-differentiated adenocarcinoma. The irregular glands in the adenocarcinoma region were formed by well-differentiated columnar cells with mild to moderate atypia and abundant cytoplasm. The nuclei were mostly located at the base and some luminal cells were stratified. When combined with proximal-type BA that had prominent flat architecture, we had difficulty distinguishing between the two components because there was no clear boundary (Fig. 1D,E). However, the tumor cells in the junctional zone between the two components had mild atypia, including intranuclear inclusions and a few sparse cilia at the top of some cells. More importantly, the basal cell layer below the epithelium lost its continuity (Fig. 1F). Immunohistochemistry (IHC) showed that the BA region of five lesions expressed P40 and cytokeratin (CK)5/6, and a continuous basal cell layer (Fig. 2A,C). P40 and CK5/6 were sporadically positive in the junctional zone between BA and LUAD, suggesting that the continuity of the basal cell layer was lost, whereas expression of P40 and CK5/6 was absent in the LUAD region (Fig. 2B). TTF1 was positive in ciliated cells and weakly positive in some basal cells, but negative in mucinous cells (Fig. 2D). Napsin-A was positive in some luminal cells in both the BA and LUAD regions (Fig. 2E,F).

Characteristics of proximal-type BA combined with IMA

One case was proximal-type BA combined with IMA. The BA region exhibited a predominance of ciliated columnar cells and columnar mucinous cells, which displayed a discontinuous jumping growth pattern along the alveolar wall and focal growth towards the luminal surface, resulting in the formation of a papillary architecture and mucous gland architecture. Additionally, the presence of morphological cavities with abundant mucinous material and a continuous basal cell layer was noted (Fig. 3A-C). There was fibrous tissue hyperplasia in the interstitium surrounding the mucinous glands. Some cancer cell nuclei were round and vacuolated, and nucleoli were prominent, similar to the morphological features of gastrointestinal adenocarcinoma (Fig. 3D). Under low magnification, there was no clear boundary between IMA and BA (Fig. 3E). Under high magnification, the glands in the junctional zone between the two components could not exclude the presence of the basal cell layer, and cilia were detectable on some luminal surfaces (Fig. 3F). CK5/6 staining showed the presence of a continuous basal cell layer in the BA area (Fig. 4A). Both CK5/6 and P40 showed sporadic positivity in the junctional zone between BA and IMA, but no expression at all in the IMA region. These findings indicated that the basal cell layer gradually lost its continuity in the junctional zone until it disappeared in the IMA region (Fig. 4B,C). TTF1 was positive in ciliated cells and weakly positive in some basal cells of the BA region, whereas mucinous cells of the BA region and IMA hardly expressed TTF1 at all (Fig. 4D,E). Napsin-A was only expressed in luminal cells of the BA region (Fig. 4F).

Characteristics of distal-type BA combined with LUAD

There were two cases of distal-type BA combined with invasive adenocarcinoma. The distal-type BA region showed predominant irregular glandular morphology covered with cuboidal cells, forming a double-layer architecture with a continuous basal cell layer. There was micropapillary-like morphology, and

Table 1. Clinicopathological characteristics of 8 patients with bronchiolar adenoma combined with lung adenocarcinoma.

Patient-Tumor	Age	Sex	Smoking History	Size (cm)	Morphology of BA	Architecture	Mucinous Cells and Cilia	Discontinuous Spread	Frozen Section Diagnosis	Final Pathological Diagnosis
1	74	F	No	0.6	Proximal	Papillary	Present	Partially Absent	minimally invasive adenocarcinoma	BA combined with AIS
2	58	F	No	1.6	Proximal	Papillary	Present	Partially Absent	minimally invasive adenocarcinoma	BA combined with AIS
3	64	F	No	1.5	Proximal	Papillary	Present	Partially Absent	BA	BA combined with minimally invasive adenocarcinoma
4	59	F	No	0.7	Proximal	Flat	Present	Partially Absent	BA	BA combined with well-differentiated adenocarcinoma
5	66	F	No	1.0	Proximal	Flat/papillary	Present	Partially Absent	LUAD	BA combined with LUAD
6	58	F	No	1.8	Proximal	Flat/papillary	Present	Partially Absent	BA	BA combined with IMA
7	52	F	No	1.2	Distal	Flat	Absent	Partially Absent	LUAD	BA combined with LUAD
8	36	F	No	0.9	Distal	Flat	Absent	Partially Absent	LUAD	BA combined with LUAD

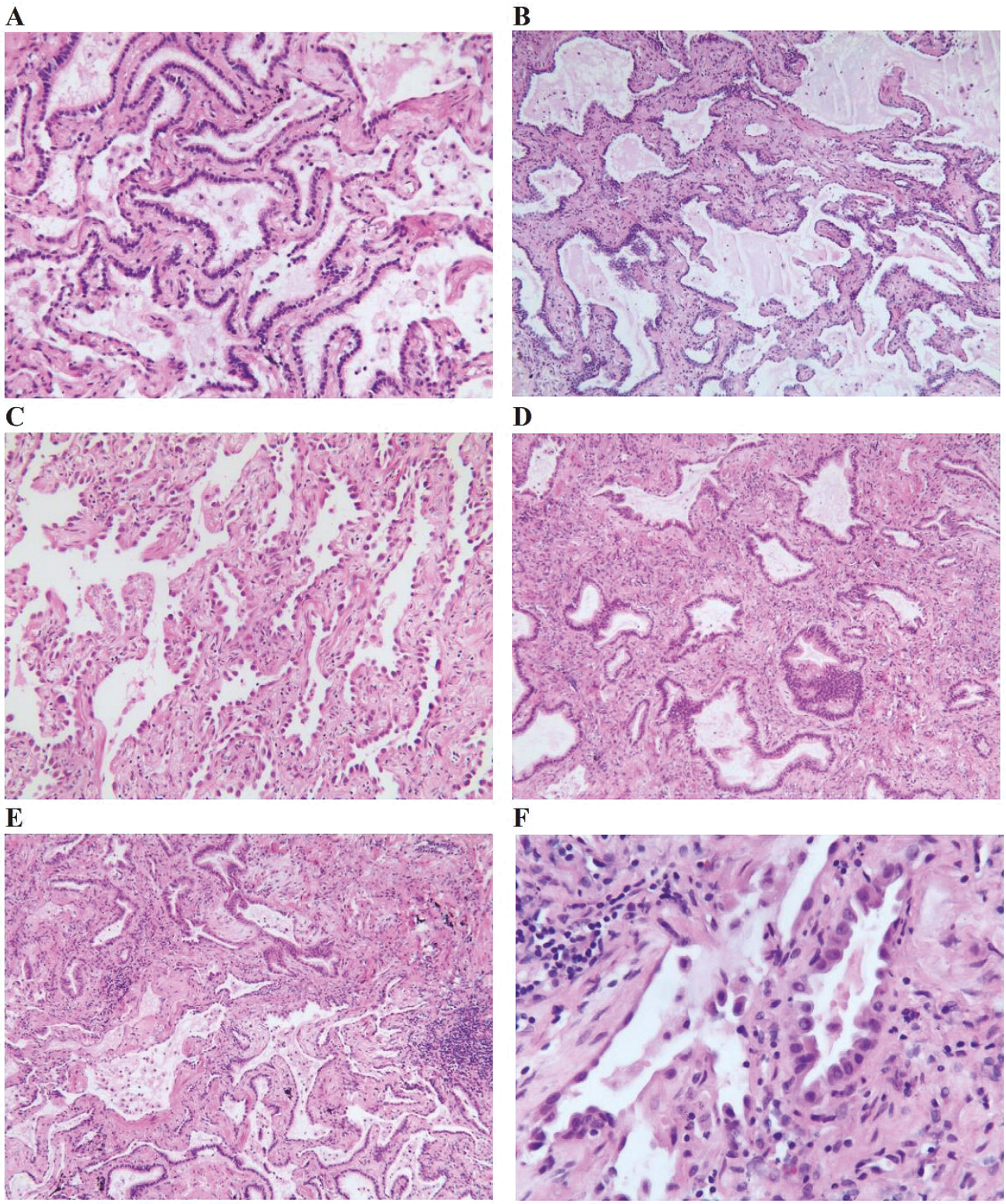

Fig. 1. Morphological characteristics of proximal-type BA combined with LUAD. **A, B.** Papillary and glandular structures of proximal-type BA. Epithelial cells were mainly ciliated columnar cells and mucous cells, and the glandular lumen was filled with mucous; a basal cell layer was visible. **C.** The region of minimally invasive adenocarcinoma showed cells with a hobnail appearance protruding into the alveolar lumen, and the invasive area was dominated by acinar structures. **D.** Areas of well-differentiated adenocarcinoma, with irregular glands composed of a single layer of columnar cells, with focal stratification and lack of a basal cell layer. **E.** The junctional zone between BA (below) and well-differentiated adenocarcinoma (above). **F.** The junctional zone epithelium was a monolayer of cuboidal epithelium with mild atypia, and intranuclear inclusions were observed. A-E, × 200; F, × 400.

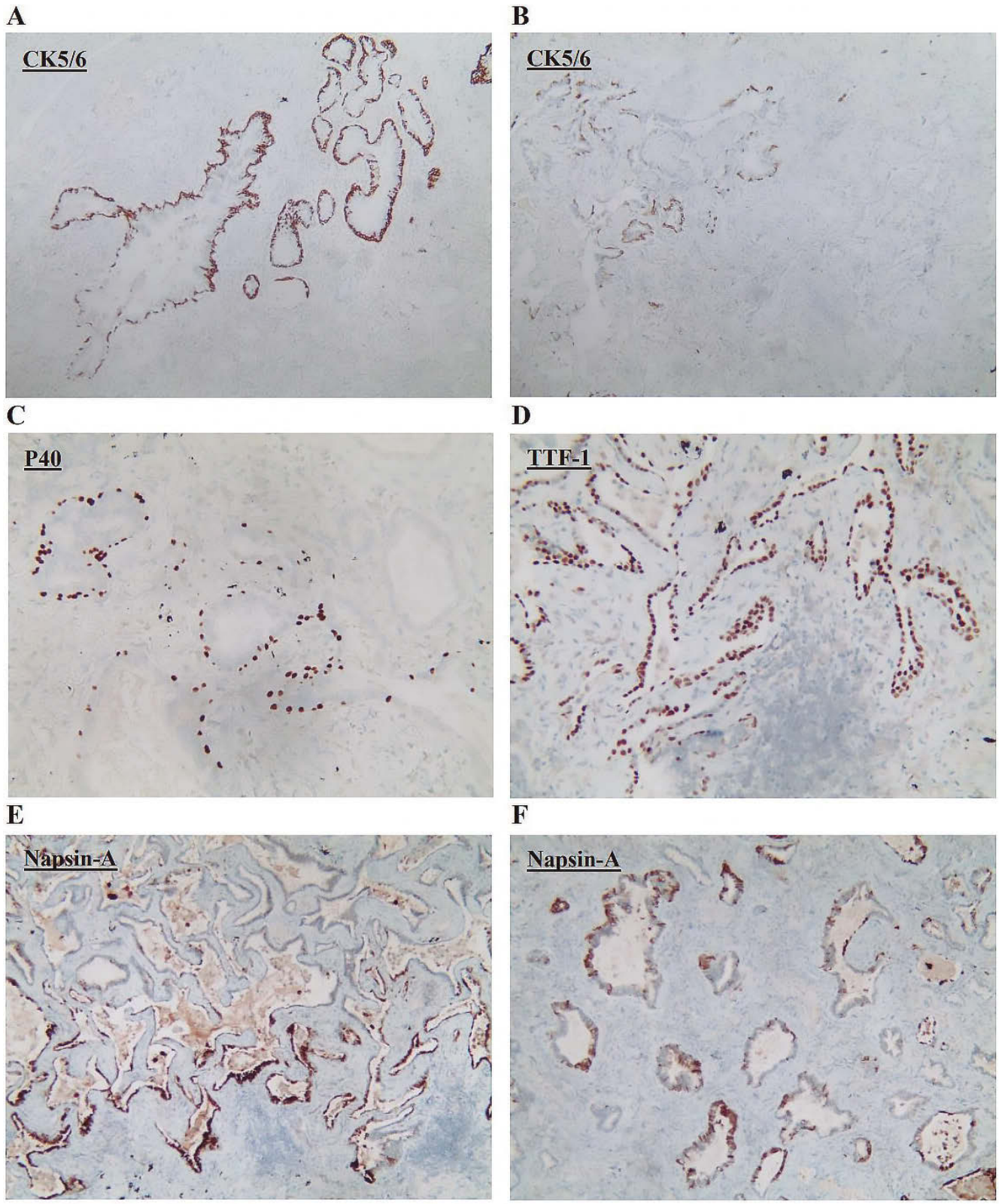

Fig. 2. Immunohistochemistry of proximal-type BA combined with LUAD. **A.** CK5/6 highlighted a continuous basal cell layer. **B.** CK5/6 showed loss of basal cell layer continuity in the BA to LUAD junction zone. LUAD region (bottom right) was CK5/6 negative. **C.** The BA region had a continuous basal cell layer expressing P40. **D.** TTF-1 was positive in ciliated cells in the BA area and weakly positive in basal cells, but was hardly expressed at all in mucous cells. **E, F.** Only some of the epithelial cells expressed Napsin-A in the BA area and LUAD region. A, C-F, × 200; B, × 50.

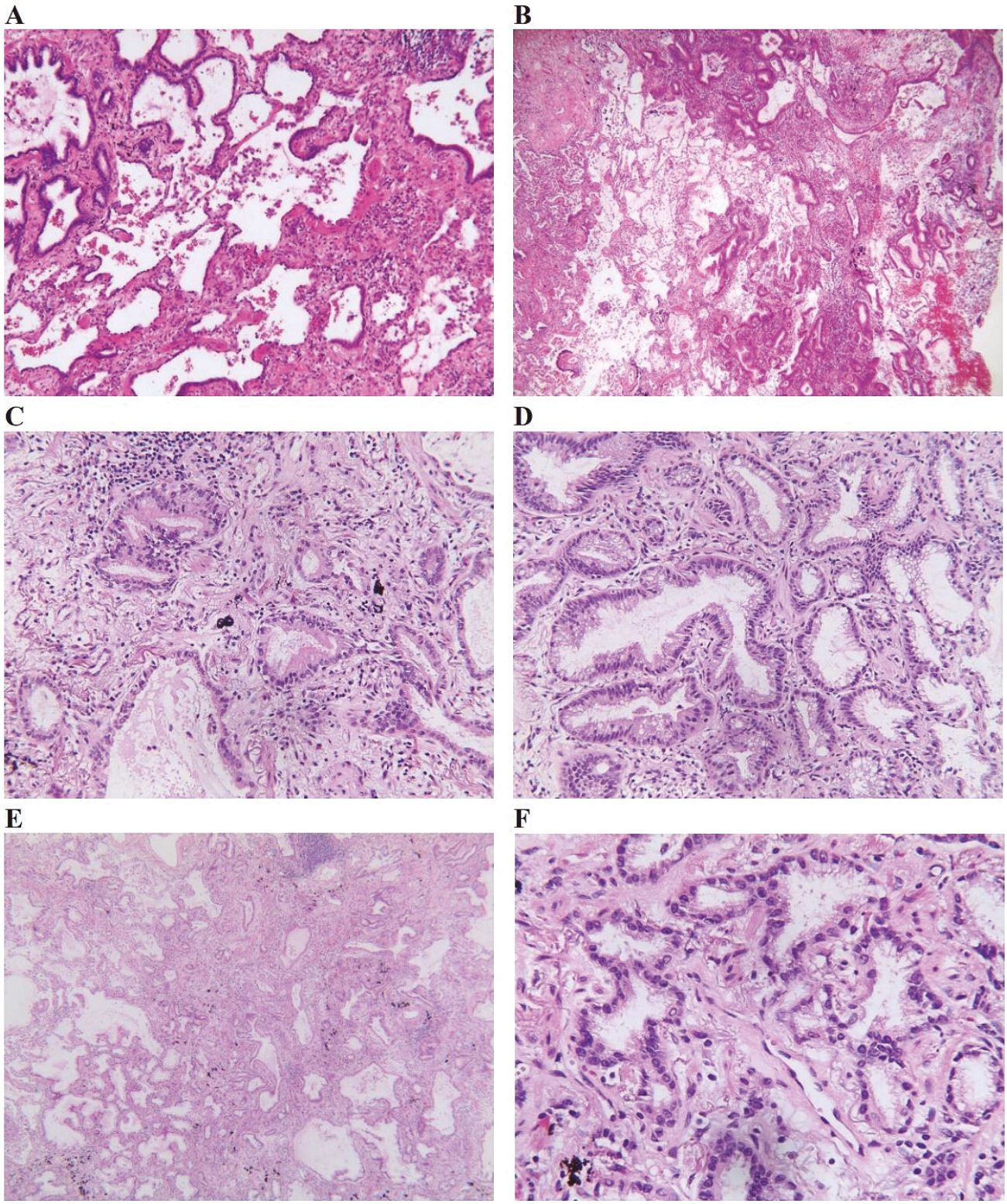

Fig. 3. Morphological characteristics of proximal-type BA with IMA. **A.** BA tumor cells displayed a discontinuous jumping growth pattern along the alveolar wall. **B.** The tumour cells exhibited comparable growth patterns in IMA region. **C.** Proximal-type BA was dominated by a flat architecture with abundant mucinous cells. Under high magnification, the tumor consisted of abundant ciliated columnar cells and mucous cells, and a continuous basal cell layer. **D.** Absence of basal cells around the glands in IMA. **E.** Under low magnification, IMA and BA had no obvious boundary. **F.** Under high magnification, the glands in the junction zone could not exclude the presence of basal cells, and cilia were visible on the surface of some epithelial cells. A, × 200; B, × 50; C, D, F, × 400; E, × 40.

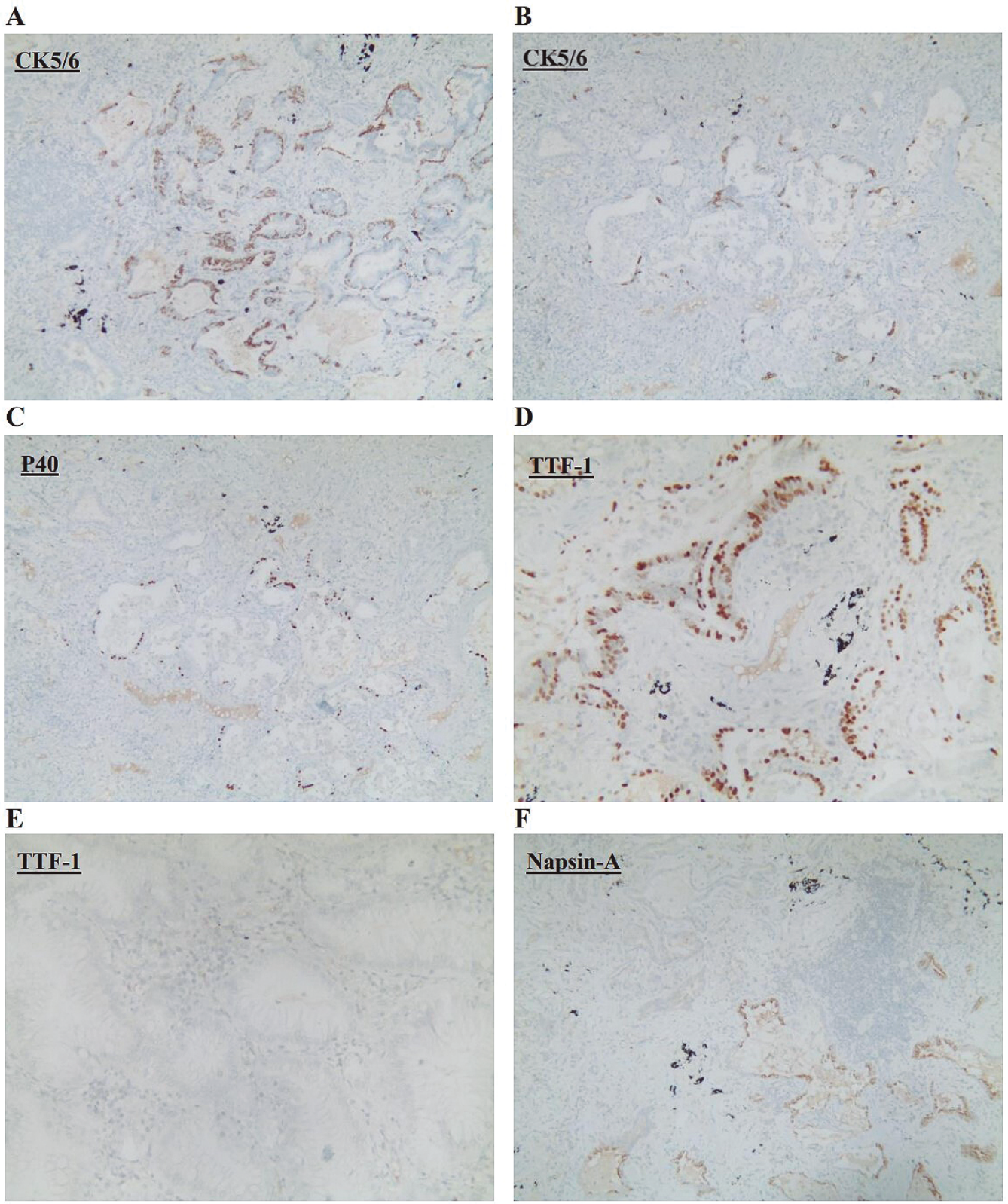

Fig. 4. Immunohistochemical phenotype of proximal-type BA combined with IMA. **A.** CK5/6 staining indicated a continuous layer of basal cells in the BA region. **B, C.** CK5/6 and P40 staining showed loss of continuity of basal cell layer in the junctional zone between BA and IMA. **D.** TTF-1 was positive in ciliated cells of BA and weakly positive in some basal cells. **E.** TTF-1 was negative in IMA. **F.** Napsin-A was only expressed in the glandular epithelium of BA (bottom right), but not in IMA (top left). A-C, F, × 200; D, E, × 400.

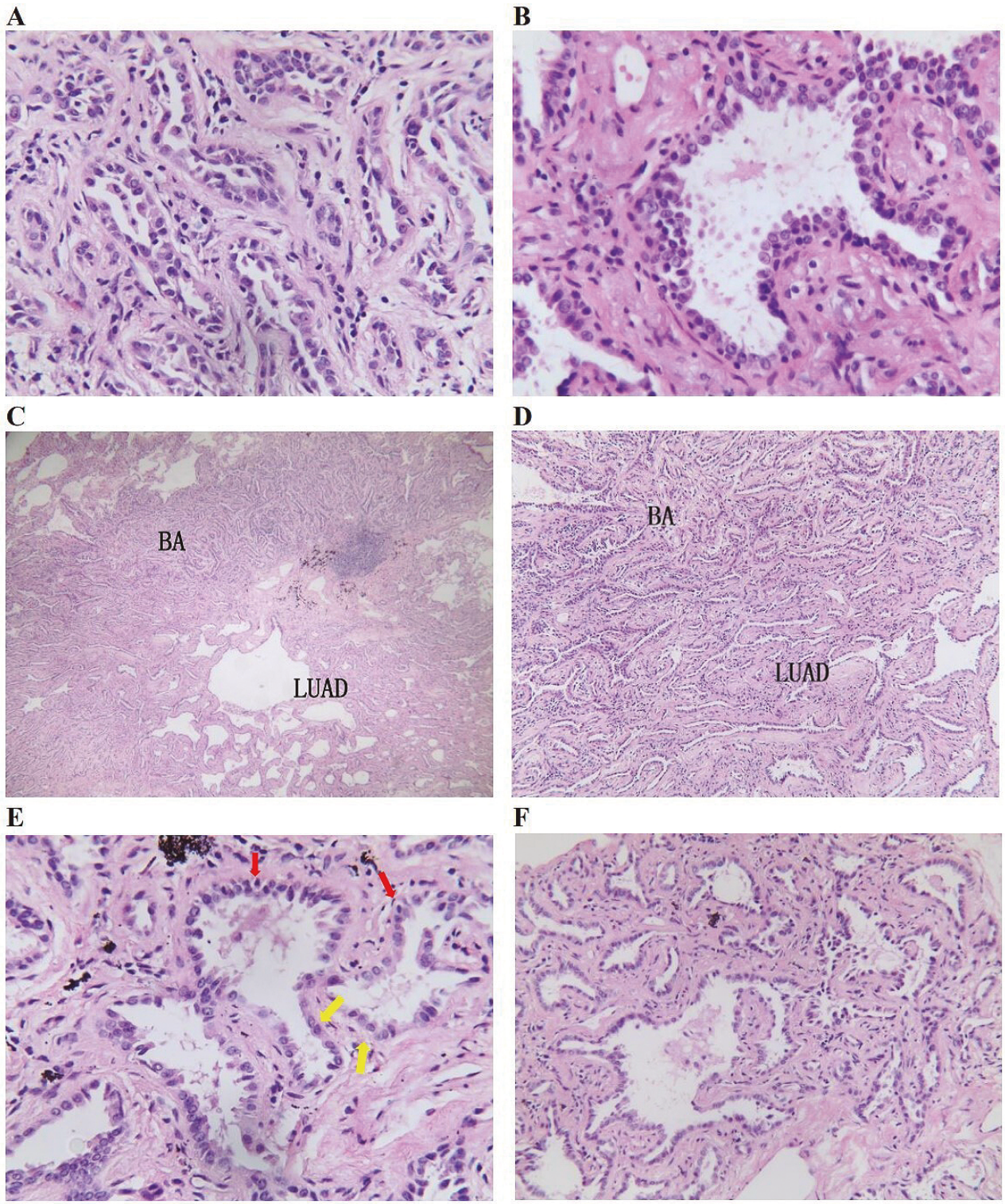

Fig. 5. Morphological characteristics of distal-type BA combined with LUAD. **A.** Distal-type BA had an almost flat structure, with cuboidal epithelial cells and a continuous layer of basal cells forming a double-layered gland, which showed complete absence of mucous cells and ciliated cells. **B.** Some cells had apical cytoplasmic snouts. **C.** Under low magnification, BA (upper left) had no clear border with LUAD (lower right). **D.** Under high magnification, the glands in the BA region had an obvious basal cell layer, while the LUAD region had glandular architecture formed by a single layer of columnar cells with significant atypia. **E.** Under high magnification, some glands in the transition zone had no continuous basal cell layer (red arrows indicate basal cells, and yellow arrows absence of basal cells), and intranuclear inclusions were observed in epithelial cells. **F.** Tumor cells in region of invasive adenocarcinoma had moderate-to-severe atypia and a basal cell layer was absent. A, B, E, F, × 400; C, × 50; D, × 200.

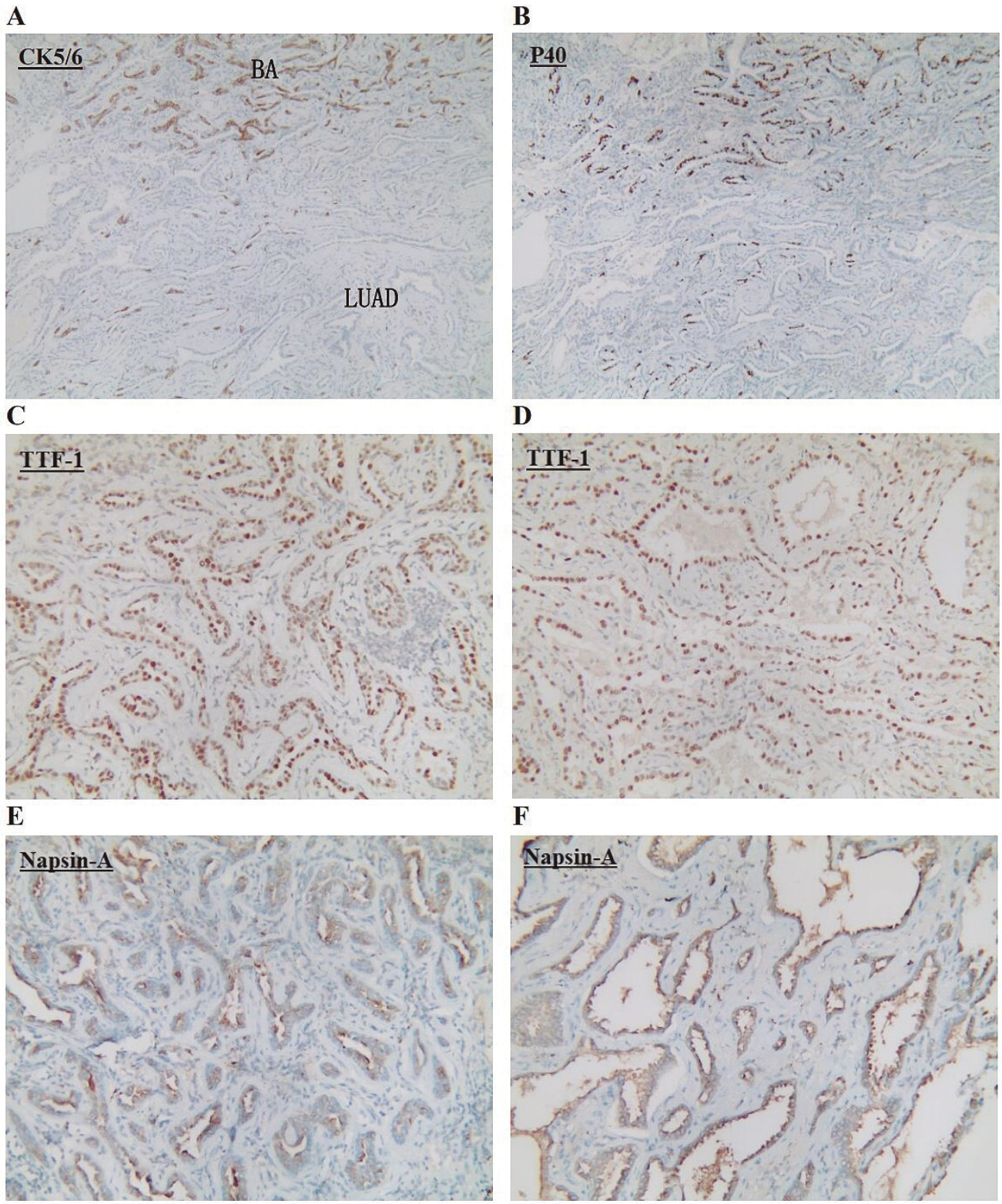

Fig. 6. Immunohistochemical phenotype of distal-type BA combined with LUAD. **A.** From the BA (upper left) to the junctional zone, and the junctional zone to the adenocarcinoma, CK5/6 staining showed progression from a continuous layer of basal cells to only scattered basal cells, and the adenocarcinoma region (lower right) had no basal cells. **B.** P40 had the same expression pattern as CK5/6. **C.** TTF-1 was positive in glandular epithelial cells of distal-type BA, and weakly positive in some basal cells. **D.** TTF-1 was positive in adenocarcinoma cells. **E.** Napsin-A was positive in glandular epithelial cells of distal-type BA, and basal cells did not express Napsin-A. **F.** Napsin-A was positive in adenocarcinoma cells. A, B, × 50; C-F, × 200.

ciliated cells and mucous cells were not visible, but some cells had apical cytoplasmic snouts (Fig. 5A,B). The BA region was also characterized by mild desmoplastic hyperplasia in the interstitium, and occasional squamous metaplasia of basal cells (Fig. 5C). Under high magnification, the LUAD region was characterized by irregular glands formed by a single layer of columnar luminal cells, in contrast to the double-layer cell architecture of the BA region (Fig. 5D). Histological features of the junctional zone between the two components included mild luminal cell atypia, visible intranuclear inclusions, and the lack of a continuous basal cell layer in some glands (Fig. 5E). LUAD dominated by glandular subtype had obvious cellular atypia, and the widening of alveolar septa was mostly a reaction of thick collagen fibers (Fig. 5F). The expression patterns of P40 and CK5/6 were the same as in the above types (Fig. 6A,B); TTF-1 was positive in luminal cells of distal type BA and LUAD cells, but weakly positive in some basal cells (Fig. 6C,D). Napsin-A was positive in luminal cells of distal-type BA and LUAD cells, while basal cells did not express Napsin-A (Fig. 6E,F).

Discussion

It is currently recognized that BA is a benign tumor arising from the pulmonary airway epithelium, from the proximal bronchioles to the surrounding alveolar structure. It is histologically characterized by a bilayer architecture with continuous basal cells (positive for p40 and CK5/6) and mild bronchiolar luminal cells (Chang et al, 2018). This feature is also the basis for the differentiation of BA from LUAD. Currently, an increasing number of studies have found that BA can have a complete loss of the basal cell layer, and comprise only a single layer of bronchiolar luminal cells. LUAD components can even coexist with BA in the same lesion, which increases the difficulty of differentiating BA from LUAD. Intraoperative frozen section examination is especially prone to misdiagnosis and missed diagnosis. BA combined with LUAD is more common in middle-aged and older people, and lacks specific clinical manifestations. The imaging features are ground-glass nodules or mixed density shadows. It has been reported that CMPT and LUAD are difficult to distinguish radiologically (Lu and Yeh, 2019; Chen et al., 2021).

In this study, we analyzed the histological and immunohistochemical phenotypic characteristics of eight cases of BA combined with LUAD. The components of BA included proximal type (n=6) and distal type (n=2). The proximal type included two types of classical BA with prominent papillary architecture, and flat type BA with glands. The two types existed alone or in combination. Their luminal surfaces were covered with a high proportion of ciliated columnar cells and mucous cells. A small amount of micropapillary morphology was observed, and the lumen contained abundant alveolar mucin. Distal-type BA was predominantly flat, with mild cuboidal cells forming the epithelium of an irregular gland. A small amount of papillary morphology was also seen, but ciliated cells and mucous cells were rare or absent. The common feature of proximal- and distal-type BA is a bilayer structure with a continuous basal cell layer. In our study, the malignant lesions in the same nodule with BA were LUAD at different stages, including AIS (n=2), minimally invasive adenocarcinoma (n=1), invasive adenocarcinoma (n=4), and IMA (n=1). There was generally no clear boundary between the two components. However, mild atypia of luminal cells and intranuclear inclusions were observed in the junctional zone between the two components. Some luminal cells showed a small number of sparse cilia or apical cytoplasmic snouts, and loss of continuity in the basal cell layer beneath the epithelium. Among the eight lesions of BA combined with LUAD, frozen section diagnosis in all cases was not completely consistent with the paraffin section diagnosis. Three of the lesions only reported BA in frozen section diagnosis, while the combined adenocarcinoma component was not visible. Conversely, the BA component was not seen in the remaining five LUAD lesions. In proximal-type BA combined with AIS or minimally invasive adenocarcinoma, the histological features of the LUAD regions included marked atypia of tumor cells with hobnail appearance protruding into the alveolar lumen, focal microinvasion, and absence of ciliated cell and basal cell layers.

The cells of BA lacked significant nuclear atypia, therefore, the key to avoiding missed diagnosis is to carefully look for ciliated cells and a continuous basal cell layer. BA, AIS and minimally invasive adenocarcinoma are treated by wedge resection; therefore, it does have different consequences for patients when frozen section diagnosis is difficult. It is worth noting that in our study, the frozen section diagnosis of one lesion was proximal-type BA because of the presence of obvious ciliated cell, mucous cell and basal cell layers. Finally, according to the morphological characteristics and IHC, we found that BA combined with well-differentiated adenocarcinoma components in the same lesion. Some lesions of distal-type BA with complete absence of ciliated cells may represent a potential diagnostic pitfall. Morphological features such as neoplastic cell atypia, visible intranuclear inclusions, or loss of basal cell layer continuity, make it necessary to consider whether BA may be combined with well-differentiated adenocarcinoma. To avoid excess surgical resection, we can only report BA for intraoperative frozen sections, but the possibility of adenocarcinoma cannot be ruled out. It is necessary to wait for paraffin sections and IHC to confirm the diagnosis. We observed that the tumor cells which displayed a discontinuous jumping growth pattern grew along the alveolar wall, and some formed papillary morphology in the lesions of proximal-type BA. Tumor cells are mainly ciliated columnar cells and mucinous cells. Because of the

similar histological features of proximal-type BA and IMA, the possibility of IMA cannot be ruled out only by the presence or absence of ciliated cells. Especially in frozen sections, the cilia of the luminal cells are blurred and difficult to identify, which makes the distinction between proximal-type BA and IMA difficult. Pathologists can look for continuous basal cell layers as a diagnostic clue, but they cannot be used as a basis for excluding any particular diagnosis. The histological morphology of paraffin sections combined with IHC should be used to make a definite diagnosis. Immunohistochemical characterization of CK5/6, P40, and P63 in the BA and LUAD regions can aid in the diagnosis.

The presence of monolayered BA-like lesions combined with LUAD complicates the diagnosis. In a recent study, Shao et al. reported 13 cases of BA lacking a continuous basal cell layer; eight consisted entirely of a monolayer of columnar or cuboidal cells, and five had a partial typical bilayer. Monolayer lesions consisting of only a single layer of columnar or cuboidal luminal cells are referred to as BA-like lesions (Shao et al., 2021). This suggests that the presence of mild cytological atypia and lack of a basal cell layer in monolayer BA-like lesions indicate that the tumor has malignant potential. Li et al. (2021) reported a case of multiple bronchiolar adenomas with malignant transformation and CCNE1 mutation, and speculated that BA may have led to carcinogenesis in some atypical cases with driver gene mutations (Li et al., 2021). Similar to the IMA combined with proximal-type BA in our study, Han et al. (2021) and Chen et al. (2021) reported a case of IMA carcinomatized by CMPT. These studies have proposed the hypothesis that CMPT is a precancerous lesion of mucinous adenocarcinoma. Han et al. (2021) reported a case of BA adjacent to IMA with KRAS mutation in both components, and suggested that the loss of continuity in the basal cell layer in the junction between BA and IMA indicated malignant transformation from BA to IMA (Han et al., 2021). Chen et al. did not detect high-frequency mutated genes associated with the occurrence of lung cancer. However, they suggested that CMPT may have been a neoplastic rather than a metaplastic process, and provided histological evidence for the hypothesis that CMPT was a precancerous lesion of mucinous adenocarcinoma. Recent studies have shown that common mutational driver genes in BA include EGFR, KRAS and BRAF. Shao et al. (2021) indicated that the overall incidence of EGFR mutations in BA patients was 52% (Shao et al., 2021), which is comparable to the 50% incidence of EGFR mutations in non-small cell lung cancer (Shi et al., 2014; Midha et al., 2015). EGFR gene mutation is associated with non-small cell lung cancer, and the high frequency of EGFR gene mutations in these reported cases suggests that BA is a neoplastic lesion. Whether BA is an early lesion associated with lung cancer is still controversial, and further large-scale investigations of similar cases are needed to confirm its malignant potential. In contrast, Chang et al. suggested that the mutational spectrum was completely different in patients with BA or BA combined with LUAD, which supports the notion that the foci of BA are not intrapulmonary spread of adenocarcinoma. Compared with the above studies, the limitation of our study was the lack of molecular studies on patients with BA or BA combined with LUAD.

In conclusion, mild cytological atypia and lack of a continuous basal cell layer were observed in the junctional zone between BA and LUAD lesions. Further study of similar cases is required to establish whether: (1) the above features represent a precancerous lesion resembling atypical adenomatous hyperplasia of the alveolar epithelium; (2) BA or monolayered BA-like lesions are atypical hyperplasia of the bronchiolar epithelium; or (3) BA or monolayered BA-like lesions will eventually become AIS or even invasive adenocarcinoma. With the in-depth study of molecular targeted therapy, our future studies will focus on the combination of morphological features and molecular genetics features. This will further improve our understanding of the pulmonary nodule and hopefully guide clinicians in the precise treatment of patients.

Acknowledgements. Not applicable.

Conflict of interest. All the authors declared that they had no conflict of interest to this work.

Funding. This work was supported by grants from the Natural Science Foundation of Jiangsu Province (BK20200201) and the National Natural Science Foundation of China (Nos. 82101215).

References

Arai Y., Shimizu S., Eimoto T., Shimizu S., Otsuki Y., Kobayashi H., Ogawa H. and Travis WD. (2010). Peripheral pulmonary papillary/glandular neoplasms with ciliated cells and a component of well-diferentiated adenocarcinoma: report of three tumours. Histopathology 56, 265-269.

Chang J.C., Montecalvo J., Borsu L., Lu S.H., Larsen B.T., Wallace W.D., Sae-Ow W., Mackinnon A.C., Kim H.R., Bowman A., Sauter J.L., Arcila M.E., Ladanyi M., Travis W.D. and Rekhtman N. (2018). Bronchiolar adenoma: expansion of the concept of ciliated muconodular papillary tumors with proposal for revised terminology based on morphologic, immunophenotypic, and genomic analysis of 25 cases. Am. J. Surg. Pathol. 42, 1010-1026.

Chen F., Ren F., Zhao H., Xu X. and Chen J. (2021). Mucinous adenocarcinoma caused by cancerization from a ciliated multinodular papilloma tumor: a case report. Thorac. Cancer 12, 1629-1633.

Han X., Hao J., Ding S., Wang E.H. and Wang L. (2021). Bronchiolar adenoma transforming to invasive mucinous adenocarcinoma: a case report. Onco. Targets Ther. 14, 2241-2246.

Li X., Wu Y., Hui D., Luo X., Wu W., Zhang J. and Chen H. (2021). Multiple bronchiolar adenomas with malignant transformation and CCNE1 mutation: a case report and literature review. J. Cardiothorac. Surg. 16, 307.

Lu Y.W. and Yeh Y.C. (2019). Ciliated muconodular papillary tumors of the lung. Arch. Pathol. Lab. Med. 143, 135-139.

Midha A., Dearden S. and McCormack R. (2015). EGFR mutation incidence in non-small-cell lung cancer of adenocarcinoma histology: a systematic review and global map by ethnicity (mutMapII). Am. J. Cancer Res. 5, 2892-2911.

Miyai K., Takeo H., Nakayama T., Obara K., Aida S., Sato K. and Matsukuma S. (2018). Invasive form of ciliated muconodular papillary tumor of the lung: a case report and review of the literature. Pathol. Int. 68, 530-535.

Shao J., Yin J.C., Bao H., Zhao R., Han Y., Zhu L, Wu X., Shao Y. and Zhang J. (2021). Morphological, immunohistochemical, and genetic analyses of bronchiolar adenoma and its putative variants. J. Pathol. Clin. Res. 7, 287-300.

Shi Y., Au J.S., Thongprasert S., Srinivasan S., Tsai C.M., Khoa M.T., Heeroma K., Itoh Y., Cornelio G. and Yang P.C. (2014). A prospective, molecular epidemiology study of EGFR mutations in Asian patients with advanced non-small-cell lung cancer of adenocarcinoma histology (PIONEER). J. Thorac. Oncol. 9, 154-162.

Wang F., Shen M.H., Cao D. and Lv J.H. (2021). Malignant ciliated muconodular papillary tumors of the lung: a case report. Int. J. Surg. Pathol. 29, 520-523.

Accepted November 29, 2023